Composites Part B 174 (2019) 106961

Contents lists available at ScienceDirect

Composites Part B

journal homepage: www.elsevier.com/locate/compositesb

Comparative analysis of micromechanical models for the elastic composite laminae

Lucas L. Vignoli [a], Marcelo A. Savi [a], Pedro M.C.L. Pacheco [b], Alexander L. Kalamkarov [c,*]

[a] Center for Nonlinear Mechanics, COPPE, Department of Mechanical Engineering, Universidade Federal do Rio de Janeiro, 21.941.972, Rio de Janeiro, P.O. Box 68.503, Brazil

[b] Department of Mechanical Engineering, Centro Federal de Educação Tecnológica Celso Suckow da Fonseca CEFET/RJ, Rio de Janeiro, RJ, Brazil

[c] Department of Mechanical Engineering, Dalhousie University, Halifax, Nova Scotia, B3H 4R2, Canada

ARTICLE INFO

Keywords:
Micromechanics
Composite material
Unidirectional lamina
Effective elastic properties

ABSTRACT

This paper deals with the first step required for the analysis and design of composite materials and structures: estimation of the effective macromechanical properties according to the structure of composite, properties of constituent materials and their volume fractions. There exist many micromechanical models proposed in the literature to estimate these effective elastic properties. Each one of these models is based on hypotheses that are valid for certain types of composite structures. The present paper aims to highlight the main assumptions of these models and compare their predictions with a set of 188 experimental data, compiled from 25 references, assuming that just the constituents' properties are available as input. The following nine major micromechanical models are evaluated: asymptotic homogenization with hexagonal unit cell; asymptotic homogenization with square unit cell; Bridging; Chamis; generalized self-consistent; Halpin-Tsai; modified Halpin-Tsai; Mori-Tanaka; and rule of mixture (ROM). Besides, a novel modified version of the rule of mixture allowing better agreement with the experimental data is also proposed. It is shown, in particular, that the newly proposed modified rule of mixture model provides the best correlation with the experimental data among the ROM-based models, while the asymptotic homogenization presents the best predictions among the elasticity-based models.

1. Introduction

Composite material design needs to define equivalent effective macromechanic properties based on information about micro constituents. Analytical, numerical and experimental approaches can be employed for this aim. The recent computational advances have increased the use of numerical approaches. Nevertheless, analytical modeling is usually more interesting as a first approach, especially in problems with many variables for optimization [1]. Experimental tests are always important, but they are related to very high costs. Besides, uncertainties related to composite structures manufacturing and measurements make this kind of analysis difficult to be effective [2]. Based on that, experimental tests are usually employed for final validations [3,4].

An additional issue for composite design is that the macromechanical stress and strain distributions are dependent on the elastic mechanical properties in anisotropic structures [5]. In other words, the homogenized properties influence the estimation of stress and strain distributions, propagating errors for further failure analysis.

The analysis from micro to macro needs the definition of a representative volume element (RVE). This definition is still objective of different approaches due to the irregular patterns of the composite material. According to Ref. [6]; the RVE "should contain sufficiently large number of fibers so that the uniformity in a statistical sense can be assumed reasonably" [7]. presented a microscopy of fiber distribution indicating that the fiber volume fraction may vary over the lamina if two different square regions are selected [8]. proposed a numerical procedure to evaluate a degree of non-uniform fiber distribution that is not possible to be represented by analytical methods [9]. proposed the use uncertainties quantification to deal with homogenization.

Based on that, there is a special motivation for critical reviews of the main micromechanics approaches, establishing a comparison with available experimental data. In this regard, the choice of the best approach depends on several aspects and there is not a definitive conclusion.

* Corresponding author.
E-mail addresses: ll.vignoli@mecanica.coppe.ufrj.br (L.L. Vignoli), savi@mecanica.coppe.ufrj.br (M.A. Savi), pedro.pacheco@cefet-rj.br (P.M.C.L. Pacheco), alex.kalamkarov@dal.ca (A.L. Kalamkarov).

https://doi.org/10.1016/j.compositesb.2019.106961
Received 30 March 2019; Received in revised form 11 May 2019; Accepted 27 May 2019
Available online 31 May 2019

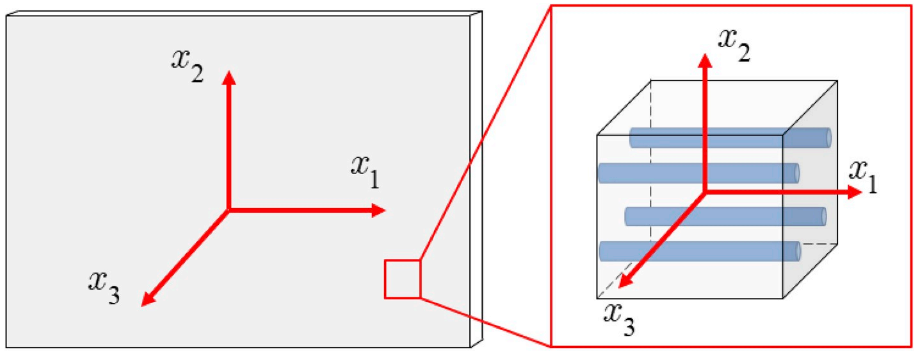

Fig. 1. Definition of coordinate systems used to define the materials properties.

Nowadays, there is an international effort to evaluate the definition of macromechanical properties from constituents' and laminae data: World Wide Failure Exercise – WWFE [10–12]. WWFE tests use conditions and lamina properties as an input, together with constituents' properties. Hence, it is not considering micromechanical homogenization as a requirement. On the conclusions of the first edition, the organizers pointed out that even the models that obtained the best predictions, presented more than 20% of the cases with error higher than 50%. During the second edition, 10% of the cases have error higher than 50% [11,13]. Therefore, there is still a considerable lack of knowledge about the estimation of different micromechanical models, mainly for transversal elastic properties and strengths.

The present paper provides a critical review of several major micromechanical models, comparing results with available experimental data. Micromechanical models are classified in two main groups: Rule of Mixture (ROM) and elasticity-based models. Specifically, nine models are analyzed: four models are based on the Rule of Mixture (ROM) [14] and five elasticity-based models [15–17]. Besides these models, a novel version of the rule of mixture is proposed, allowing better agreement with the experimental data. The goal of this comparison is to evaluate the best model performances, evaluating the more representative assumptions of a real composite structure. This study evaluates the reliability of the micromechanical models for the elastic properties of a composite structure. The classification proposed in the present paper is not the only possibility, see e.g., Refs. [18–20].

Recently [21,22], presented review articles related to effective properties of unidirectional laminae [21]. compared the models with 6 experimental data of glass fiber composite. On the other hand [22], investigated strength properties with limited experimental data. The major contribution of the present study when compared with this other two review articles is a broader comparison using more experimental data and ten analytical models, including a novel modification of the ROM. Note that only unidirectional laminae are considered; for bidirectional composites some additional issues must be evaluated, as discussed in Refs. [23,24].

Curvilinear composite shells with different surface reinforcements were considered earlier, see Refs. [16,17,25–27]. The modified asymptotic homogenization technique was developed in these works and applied for calculating the effective moduli Aij, Bij, Dij of the reinforced composite shells. The comparison of the results of asymptotic homogenization model and more simplified approaches was also performed in the above studies, and it was demonstrated that asymptotic homogenization provides more accurate results.

This introduction presents the fundamental definitions for the rest of the paper. After this introduction, Section 2 presents the five ROM-based models, including the own ROM and the novel modification proposed. Sections 3 presents the five elasticity-based models; in this section the major assumptions of each models are introduced, but a detailed derivation is omitted. Section 4 presents the calibration of the novel ROM-based model as well as comparison of the models estimations with a set of experimental data compiled on the literature. At last, in Section 5 the main conclusions are highlighted, and some recommendations are pointed out.

1.1. Fundamentals

Before starting the micromechanical model analysis, some general considerations are introduced. Fig. 1 presents an isotropic plane of lamina and fibers, where direction x_1 is parallel to the longitudinal fiber direction.

The composite material is assumed to be a linear elastic unidirectional transversally isotropic lamina. The fibers are assumed to be transversally isotropic and the matrix isotropic. Under these assumptions, the composite material has five independent properties: longitudinal and transversal elastic modulus (E_1 and E_2); in-plane and out-of-plane shear modulus (G_{12} and G_{23}); and in-plane Poisson's ratio (ν_{12}). These macromechanical properties are defined from the properties of the constituent materials. It is considered that superscript f is used to represent fiber property while m is employed to characterize matrix property. Therefore, E_1^f, E_2^f, G_{12}^f, G_{23}^f, ν_{12}^f are fiber properties (longitudinal elastic modulus, transversal elastic modulus, in-plane shear modulus, out-of-plane shear modulus and in-plane Poisson's ratio, respectively); and E^m, ν^m, $G^m = E^m/2(1+\nu^m)$ are matrix properties (elastic modulus, Poisson's ratio and shear modulus). Another important definition to characterize a composite material is the volume fraction of each one of the constituents: V_f is the fiber volume fraction while V_m is the matrix volume fraction. Another possibility is the consideration of void volume fractions, V_v. In any case, the sum of the volume fractions needs to be 1: $V_m + V_f + V_v = 1$.

It should be pointed out that although five independent elastic properties are required for the full characterization of the lamina, some models are not able to estimate all of them.

2. Models based on the rule of mixture

The rule of mixture is an intuitive homogenization approach that becomes popular due to its simplicity. In order to increase the prediction capability, some modifications were proposed based on different approaches. These theories are very convenient due to simplicity and practical issues, and the modifications of the ROM are usually based on experimental or numerical data to fit the curves. Empirical formulas are generally employed in order to obtain better experimental predictions. This section presents a general overview of some of the models based on the ROM. Besides, a novel model is proposed considering a new adjustment based on experimental data.

2.1. Rule of mixture (ROM)

The Rule of Mixtures is based on a straight solid mechanics analysis assuming that fibers and matrix may be modeled as elements in parallel or in series, according to the applied load. The equations to estimate the in-plane properties by the ROM are given by (see, e.g. Ref. [28],

$$E_1 = E_1^f V_f + (1 - V_f) E^m \quad (1)$$

$$\nu_{12} = \nu_{12}^f V_f + (1 - V_f) \nu^m \quad (2)$$

$$E_2 = \frac{E_2^f E^m}{E_2^f (1 - V_f) + E^m V_f} \quad (3)$$

$$G_{12} = \frac{G_{12}^f G^m}{G_{12}^f (1 - V_f) + G^m V_f} \quad (4)$$

The plane strain bulk modulus is an additional property estimated considering a biaxial load transversally to the fibers, and therefore, the elements may also be assumed in parallel (see, e.g. Ref. [29],

$$K_{23} = \frac{K_{23}^f K^m}{K_{23}^f (1 - V_f) + K^m V_f} \quad (5)$$

where K_{23}^f and K^m are the fiber and matrix bulk moduli. The following expressions are useful to establish a relation between the plane strain bulk modulus and the other properties and also to compute the out-of-plane shear modulus

$$K_{23} = \frac{\mathrm{E}_1}{4\left[(\mathrm{E}_1/\mathrm{E}_2) - \nu_{12}^2\right] - (\mathrm{E}_1/G_{23})} \quad (6)$$

$$G_{23} = \frac{\mathrm{E}_1}{4\left[(\mathrm{E}_1/\mathrm{E}_2) - \nu_{12}^2\right] - (E_1/K_{23})} \quad (7)$$

Since the predictions of E_1 and ν_{12} are usually close to experimental data, most of the models uses the same approach for that. Nevertheless, the other property predictions, transversal and shear properties, need to be improved and this motivate different descriptions that are presented in the sequence. Hence, in the absence of explicit comment, the ROM-based models use the same equations, Eq. (1) and Eq. (2), to estimate E_1 and ν_{12}, respectively.

2.2. Chamis (Ch) model

[30] proposed the inclusion of the effect of the voids content on the prediction of equivalent properties. Besides, nonlinear influence of the fiber volume fraction on the transversal properties is adopted. Based on that, the following equations are employed

$$E_1 = E^m + (1 - V_v) V_f \left(E_1^f - E^m\right) \quad (8)$$

$$E_2 = \frac{E^m}{1 - \sqrt{(1 - V_v) V_f}\left[1 - \left(E^m/E_2^f\right)\right]} \quad (9)$$

$$G_{12} = \frac{G^m}{1 - \sqrt{(1 - V_v) V_f}\left[1 - \left(G^m/G_{12}^f\right)\right]} \quad (10)$$

$$G_{23} = \frac{G^m}{1 - \sqrt{(1 - V_v) V_f}\left[1 - \left(G^m/G_{23}^f\right)\right]} \quad (11)$$

$$\nu_{12} = \nu^m + (1 - V_v) V_f \left(\nu_{12}^f - \nu^m\right) \quad (12)$$

Note that if the microstructural voids are neglected ($V_v = 0$), the Chamis model becomes closer to the Rule of Mixture: the main difference is the estimation for G_{23} and to replace V_f by $\sqrt{V_f}$ for E_2 and G_{12}.

[31] suggested an inverse modeling approach; first the laminate properties are measured and then these quantities are used to compute the constituents' properties. This methodology is useful to avoid issues on the fibers' properties measure. On the other hand, it carries error from the micromechanical model [32]. also suggested the use of an inverse methodology.

2.3. Halpin-Tsai (HT) and modified Halpin-Tsai (HTm) models

[33] suggested the following set of equations different of the ROM:

$$E_2 = E^m \left(\frac{1 + \zeta_{E_2} \eta_{E_2} V_f}{1 - \eta_{E_2} V_f}\right) \quad (13)$$

$$G_{12} = G^m \left(\frac{1 + \zeta_{G_{12}} \eta_{G_{12}} V_f}{1 - \eta_{G_{12}} V_f}\right) \quad (14)$$

where

$$\eta_{E_2} = \frac{\left(E_2^f/E^m\right) - 1}{\left(E_2^f/E^m\right) + \zeta_{E_2}} \quad (15)$$

$$\eta_{G_{12}} = \frac{\left(G_{12}^f/G^m\right) - 1}{\left(G_{12}^f/G^m\right) + \zeta_{G_{12}}} \quad (16)$$

Moreover, ζ_{E_2} and $\zeta_{G_{12}}$ are parameter than can be calibrated using experimental data. A general recommendation to be use when there is not experimental data for calibration is presented in the sequence [34].

$$\zeta_{E_2} = 2 + 40 {V_f}^{10} \quad (17)$$

$$\zeta_{G_{12}} = 1 + 40 {V_f}^{10} \quad (18)$$

Recently, a modified Halpin-Tsai (HTm) model is proposed by Ref. [35] based in a parametric finite element study considering a broad possibility of random fiber arrangement,

$$\zeta_{E_2} = \begin{cases} 4.924 - 35.888 V_f + 125.118 {V_f}^2 - 145.121 {V_f}^3 & if \quad V_f < 0.3 \\ 1.5 + 5500 {V_f}^{18} & if \quad V_f \geq 0.3 \end{cases} \quad (19)$$

2.4. Modified rule of mixture (ROMm)

A novel modified ROM is proposed in the present Section. It is based on introduction of adjustable parameters allowing better agreement with the experimental data. This adjustment must contain not only the fiber volume fraction, as the Halpin-Tsai model, but also the ratio between matrix and fiber properties. Besides, three main assumptions are considered: the ROM is employed for the estimation of E_2 and G_{12}; the Chamis model is employed to estimate G_{23}, but using V_f instead of $\sqrt{V_f}$. The basic equations are the following:

$$E_2 = E^m \left(\frac{1}{1 + \xi_{E_2}\left[\left(E^m/E_2^f\right) - 1\right] V_f}\right) \quad (20)$$

$$G_{12} = G^m \left(\frac{1}{1 + \xi_{G_{12}}\left[\left(G^m/G_{12}^f\right) - 1\right] V_f}\right) \quad (21)$$

$$G_{23} = G^m \left(\frac{1}{1 + \xi_{G_{23}}\left[\left(G^m/G_{23}^f\right) - 1\right] V_f}\right) \quad (22)$$

where ξ_{E_2}, $\xi_{G_{12}}$, $\xi_{G_{23}}$ are the experimental adjustment parameters. Note that if $\xi_{E_2} = 1$ and $\xi_{G_{12}} = 1$, Eqs. 20 and 21 are equals to Eq.(3) and (4). These quantities are defined by

$$\xi_{E_2} = \left[x_1 + x_2 V_f + x_3 \left(E^m/E_2^f\right)\right] \quad (23)$$

$$\xi_{G_{12}} = \left[x_4 + x_5 V_f + x_6 \left(G^m/G_{12}^f\right)\right] \quad (24)$$

$$\xi_{G_{23}} = \left[x_7 + x_8 V_f + x_9 \left(G^m/G_{23}^f\right)\right] \quad (25)$$

where x_i are calibrated according to experimental data.

Note that, based on Eqs. 20–22, the effective properties (transversal elastic modulus, in-plane and out-of-plane shear moduli) are equal to the matrix properties multiplied by a function of the fiber volume fraction and the ratio between matrix and fiber properties. Based on this observation, Eqs. 23–25 are proposed where the parameters ξ with different subscripts represent a linear combination of the fiber volume fraction and the ratio between matrix and fiber properties.

The calibration of the novel ROMm employs the Levenberg-Marquardt algorithm [36] to minimize the error between the model estimative and the experimental data. The calibrated parameters and the list of references compiled with experimental data are presented in Section 4.

3. Models based on the theory of elasticity

Several elasticity-based solutions have been proposed to estimate macromechanical properties for composite materials. These approaches include upper and lower bands from variational approaches [37]. presented a rigorous discussion about the terminology found in the literature. These authors highlighted that: "'constructive solution' and more strong 'exact formula' are not acceptable when one writes a formula when its entries could be found from an additional numerical procedure"; "closed form solution usually excludes usage of series"; and "asymptotic formulae can be considered as analytical approximations". Investigate the source of these misunderstanding terms is not the aim of the present investigation, but, in the authors' opinion, the critical essay presented by Ref. [37] should be cited.

The goal of this Section is to present a brief introduction to the elasticity-based models, including their main assumptions and equations. Results of application of these models are compared with the experimental data in the next Section.

3.1. Generalized self consistent model (GSCM)

The GSCM assumes that a simple unit cell may properly represent the microstructure: a fiber embedded in a matrix, forming two concentric cylinders, in such way that $V_f \cong (R_f/R)^2$, where R_f and R are the radius of the fiber and of the external cylinder that represents the matrix, respectively. Around the matrix cylinder, there exist an infinite body that has the same properties than the assembly fiber-matrix. A detailed discussion about this model is presented by Refs. [38,39].

The complete set of equations for this model is obtained by assuming three different load conditions: a triaxial load with $\langle\sigma_{11}\rangle = \tilde{\sigma}_L$ and $\langle\sigma_{22}\rangle = \langle\sigma_{33}\rangle = \tilde{\sigma}_T$; in-plane and out-of-plane shear loads, where $< \ldots >$ means the average value. Just the first one is presented here to introduce the idea of this model. For the triaxial load, the non-null displacement components of the unit cell are

$$u_1 = \varepsilon_{11}x_1 \tag{26}$$

$$u_r = \begin{cases} \alpha_1 r & \text{if} \quad 0 \le r \le R_f \\ \alpha_2 r + \dfrac{\alpha_3}{r} & \text{if} \quad R_f \le r \le R \end{cases} \tag{27}$$

where α_i are constants obtained using the constitutive relations of the constituents and the strain definitions for small deformation in cylindrical coordinate system satisfying the following boundary conditions [40],

$$u_r^f(r=R_f) = u_r^m(r=R_f) \tag{28}$$

$$\sigma_{rr}^f(r=R_f) = \sigma_{rr}^m(r=R_f) \tag{29}$$

$$\sigma_{rr}^m(r=R) = \tilde{\sigma}_T \tag{30}$$

For a uniaxial load, $\langle\sigma_{22}\rangle = \langle\sigma_{33}\rangle = \tilde{\sigma}_T = 0$ and $E_1 = \langle\sigma_{11}\rangle / \langle e_{11}\rangle$. Hence, it is possible to obtain

$$E_1 = E_1^f V_f + E^m(1-V_f) + \frac{4V_f(1-V_f)(\nu_{12}^f - \nu^m)^2}{\frac{(1-V_f)}{K_{23}^f} + \frac{V_f}{K_{23}^m} + \frac{1}{G^m}} \tag{31}$$

By using the Poisson's ratio definition, $\nu_{12} = -e_{rr}(r=R)/e_{11}$, leads to the following equation

$$\nu_{12} = \nu_{12}^f V_f + \nu^m(1-V_f) + \frac{V_f(1-V_f)(\nu_{12}^f - \nu^m)\left(\frac{1}{K_{23}^m} - \frac{1}{K_{23}^f}\right)}{\frac{(1-V_f)}{K_{23}^f} + \frac{V_f}{K_{23}^m} + \frac{1}{G^m}} \tag{32}$$

Alternatively, for plane-strain ($\varepsilon_{11} = 0$), with a similar procedure, the plane strain bulk modulus is obtained

$$K_{23} = K_{23}^m + \frac{V_f}{\frac{1}{K_{23}^f - K_{23}^m} + \frac{1-V_f}{K_{23}^m + G^m}} \tag{33}$$

The other additional properties are computed by

$$G_{12} = G^m \frac{G_{12}^f(1+V_f) + G^m(1-V_f)}{G_{12}^f(1-V_f) + G^m(1+V_f)} \tag{34}$$

$$G_{23} = G^m\left(\frac{-B + \sqrt{B^2 - 4AC}}{2A}\right) \tag{35}$$

where

$$A = a_0 + a_1 V_f + a_2 V_f^2 + a_3 V_f^3 + a_4 V_f^4 \tag{36}$$

$$B = b_0 + b_1 V_f + b_2 V_f^2 + b_3 V_f^3 + b_4 V_f^4 \tag{37}$$

$$C = c_0 + c_1 V_f + c_2 V_f^2 + c_3 V_f^3 + c_4 V_f^4 \tag{38}$$

$$a_0 = -2(G^m)^2(2G^m + K^m)[2G_{23}^f G^m + K_{23}^f(G_{23}^f + G^m)][2G_{23}^f G^m + K^m(G_{23}^f + G^m)] \tag{39}$$

$$a_1 = 8(G^m)^2(G_{23}^f - G^m)[2G_{23}^f G^m + K_{23}^f(G_{23}^f + G^m)][(G^m)^2 + G^m K^m + (K^m)^2] \tag{40}$$

$$= -12(G^m)^2(K^m)^2(G_{23}^f - G^m)[2G_{23}^f G^m + K_{23}^f(G_{23}^f + G^m)] \tag{41}$$

$$\begin{aligned} = 8(G^m)^2\Big\{&(G_{23}^f G^m)^2 K_{23}^f + (G_{23}^f)G^m K^m(K_{23}^f - G^m) \\ &+ (K^m)^2[G_{23}^f G^m(G_{23}^f - 2G^m) + K_{23}^f(G_{23}^f - G^m)(G_{23}^f + G^m)]\Big\} \end{aligned} \tag{42}$$

$$a_4 = 2(G^m)^2(G_{23}^f - G^m)(2G^m + K^m)[K_{23}^f G^m K^m - G_{23}^f(2G^m(K_{23}^f - K^m) + K_{23}^f K^m)] \tag{43}$$

$$b_0 = 4(G^m)^3[2G_{23}^f G^m + K_{23}^f(G_{23}^f + G^m)][2G_{23}^f G^m + K^m(G_{23}^f + G^m)] \tag{44}$$

$$b_1 = 8(G^m)^2 K^m(G_{23}^f - G^m)[2G_{23}^f G^m + (G_{23}^f + G^m)K_{23}^f](G^m - K^m) \tag{45}$$

$$b_2 = -2a_2 \tag{46}$$

$$b_3 = -2a_3 \tag{47}$$

$$b_4 = -4(G^m)^3(G_{23}^f - G^m)\{K_{23}^f G^m K^m - G_{23}^f[2G^m(K_{23}^f - K^m) + K_{23}^f K^m]\} \tag{48}$$

$$c_1 = 8(G^m K^m)^2(G_{23}^f - G^m)[2G_{23}^f G^m + K_{23}^f(G_{23}^f + G^m)] \tag{49}$$

$$c_2 = a_2 \tag{50}$$

$$c_3 = a_3 \tag{51}$$

$$c_4 = -2(G^m)^2 K^m \left(G_{23}^f - G^m\right)\left\{K_{23}^f G^m K^m - G_{23}^f\left[2G^m\left(K_{23}^f - K^m\right) + K_{23}^f K^m\right]\right\} \tag{52}$$

3.2. Mori-Tanaka model (MT)

The Mori-Tanaka model [41,42] is based on the Eshelby inclusion theory using the eigenstrain concept [43]. The idea is to establish an average behavior defined from fiber and matrix behaviors. Hence, the stress, σ_{ij}, and strain, ε_{ij}, tensors can be defined from their average values, evaluated on matrix and fibers [44],

$$\langle\sigma_{ij}\rangle = \frac{1}{V}\int \sigma_{ij} dv = V_f\left\langle\sigma_{ij}^{(f)}\right\rangle + (1 - V_f)\left\langle\sigma_{ij}^{(m)}\right\rangle \tag{53}$$

$$\langle e_{ij}\rangle = \frac{1}{V}\int e_{ij} dv = V_f\left\langle e_{ij}^{(f)}\right\rangle + (1 - V_f)\left\langle e_{ij}^{(m)}\right\rangle \tag{54}$$

The essential assumption for macroscopic homogenization is to establish a relationship between the average stress and the average strain tensors by effective elastic tensor $\tilde{c}_{ijkl}$, allowing one to write equivalent constitutive relation $\langle\sigma_{ij}\rangle = \tilde{c}_{ijkl}\langle e_{kl}\rangle$. Considering that constituents are linear and elastic, it is possible to write average equations for fibers and matrix, $\langle\sigma_{ij}^{(f)}\rangle = c_{ijkl}^{(f)}\langle e_{kl}^{(f)}\rangle$ and $\langle\sigma_{ij}^{(m)}\rangle = c_{ijkl}^{(m)}\langle e_{kl}^{(m)}\rangle$, where the elastic tensors of both phases are known. By assuming that there exist a fourth-order tensor T_{ijkl}, which relates fiber and matrix strains, $\langle e_{ij}^{(f)}\rangle = T_{ijkl}\langle e_{kl}^{(m)}\rangle$, the following expression are obtained with tensor manipulation

$$\tilde{c}_{ijkl} = c_{ijkl}^{(m)} + V_f\left(c_{ijpq}^{(f)} - c_{ijpq}^{(m)}\right)T_{pqmn}\left[(1 - V_f)I_{mnkl} + V_f T_{mnkl}\right]^{-1} \tag{55}$$

Tensor T_{ijkl} can be calculated using the Eshelby inclusion principle that leads to,

$$T_{ijkl} = \left[I_{ijkl} - S_{ijmn}\left(c_{\text{mnpq}}^{(m)}\right)^{-1}\left(c_{pqkl}^{(m)} - c_{pqkl}^{(f)}\right)\right]^{-1} \tag{56}$$

where S_{ijkl} is the fourth-order Eshelby tensor that depends on the matrix properties and inclusion geometry shape. A set of generic solutions for isotropic and anisotropic matrix is found in Ref. [43].

According to Ref. [45]; the longitudinal and transverse elastic moduli, in-plane Poisson's ratio, in-plane and out-of-plane shear moduli are computed with the following equations,

$$E_1 = V_f E_1^f + (1 - V_f)E_m + 2V_f(1 - V_f)Z_1\left(\nu_{12}^f - \nu^m\right)^2 \tag{57}$$

$$E_2 = \frac{E_1}{\left[1 - (\nu^m)^2\right](Y_1 + Y_2)} \tag{58}$$

$$\nu_{12} = \nu^m + 2V_f\frac{Z_1}{E^m}\left(\nu_{12}^f - \nu_m\right)\left[1 - (\nu^m)^2\right] \tag{59}$$

$$G_{12} = \frac{E^m}{2(1 - V_f)(1 + \nu^m)}\left[1 + V_f - \frac{4V_f}{1 + V_f + 2(1 - V_f)\frac{G_{12}^f}{E^m}(1 + \nu^m)}\right] \tag{60}$$

$$G_{23} = E^m\left\{2(1 + \nu^m) + \frac{V_f}{\frac{1 - V_f}{8[1 - (\nu^m)^2]} + \frac{G_{23}^f}{E^m - 2G_{23}^f(1 + \nu^m)}}\right\}^{-1} \tag{61}$$

where

$$Y_1 = V_f Z_1\left(\frac{E_1^f}{E^m}\right)\left[\frac{1 + \nu^m}{E^m} - \frac{2}{E_1^f} + \frac{1 + \nu_{23}^f}{E_2^f}\right] \tag{62}$$

$$Y_2 = \frac{1}{1 - (\nu^m)^2} + 2V_f\left(\frac{E_1}{Z_2}\right)\left[1 + \nu_{23}^f - \frac{E_2^f}{E^m}(1 - \nu^m)\right] \tag{63}$$

$$Z_1 = \left\{-2(1 - V_f)\frac{\left(\nu_{23}^f\right)^2}{E_1^f} + (1 - V_f)\frac{1 - \nu_{23}^f}{E_2^f} + \frac{(1 + \nu^m)\left[1 + V_f(1 - 2\nu^m)\right]}{E^m}\right\}^{-1} \tag{64}$$

$$Z_2 = E_2^f(3 + V_f - 4\nu^m)(1 + \nu^m) + (1 - V_f)E^m\left(1 + \nu_{23}^f\right) \tag{65}$$

3.3. Bridging model (Br)

Bridging model defines a relation between matrix and fiber stress tensors using a fourth-order bridging tensor A_{ijkl}, written as follows [46]:

$$\left\langle\sigma_{ij}^{(m)}\right\rangle = A_{ijkl}\left\langle\sigma_{kl}^{(f)}\right\rangle \tag{66}$$

Using Mori-Tanaka model as basis, the effective elastic tensor of the composite is computed by

$$\tilde{c}_{ijkl} = \left[(1 - V_f)A_{ijpq} + V_f I_{ijpq}\right]D_{pqkl}^{-1} \tag{67}$$

where $D_{ijkl} = (1 - V_f)s_{ijpq}^{(m)}A_{pqkl} + V_f s_{ijkl}^{(f)}$ and $s_{ijkl}^{(m)}$ and $s_{ijkl}^{(f)}$ are the compliance tensors.

Therefore, Eq. (70) can be employed to estimate effective elastic tensor after the determination of the bridging tensor [47]. proposed an alternative solution based on the concentric cylinders model. Using the contracted notation to represent a fourth-order tensor as a 6×6 matrix, the bridging tensor non-null components are given by

$$[A]_{11} = \frac{E^m}{E_1^f}\left[1 + \frac{\nu^m(\nu^m - \nu_{12}^f)}{(1 + \nu^m)(1 - \nu^m)}\right] \tag{68}$$

$$[A]_{12} = [A]_{13} = \frac{1}{(1 - \nu^m)}\left\{\frac{E^m}{(1 + \nu^m)}\left[\frac{\nu^m(1 - \nu_{23}^f)}{2E_2^f} - \frac{\nu_{12}^f}{E_1^f}\right] + \frac{\nu^m}{2}\right\} \tag{69}$$

$$[A]_{21} = [A]_{31} = \frac{E^m}{2E_1^f}\frac{(\nu^m - \nu_{12}^f)}{(1 + \nu^m)(1 - \nu^m)} \tag{70}$$

$$[A]_{22} = [A]_{33} = \frac{1}{(\nu^m - 1)(\nu^m + 1)}\left\{E^m\left[\frac{(\nu_{23}^f - 3)}{8E_2^f} + \frac{\nu^m\nu_{12}^f}{2E_1^f}\right] + \frac{(\nu^m + 1)(4\nu^m - 5)}{8}\right\} \tag{71}$$

$$[A]_{32} = [A]_{23} = \frac{1}{(1 - \nu^m)(1 + \nu^m)}\left\{E^m\left[\frac{(3\nu_{23}^f - 1)}{8E_2^f} + \frac{\nu^m\nu_{12}^f}{2E_1^f}\right] + \frac{(\nu^m + 1)(1 - 4\nu^m)}{8}\right\} \tag{72}$$

$$[A]_{44} = \frac{G^m}{4G_{23}^f(1 - \nu^m)} + \frac{(3 - 4\nu^m)}{4(1 - \nu^m)} \tag{73}$$

$$[A]_{55} = [A]_{66} = \frac{G^m + G_{12}^f}{2G_{12}^f} \tag{74}$$

Despite Eq.68–74 are the elasticity solution of the Bridging tensor [47], presented some results indicating that the simplified version presented by Ref. [48] is able to obtain a better fit with experimental data

$$E_1 = E_1^f V_f + (1 - V_f)E^m \tag{75}$$

$$\nu_{12} = \nu_{12}^f V_f + (1 - V_f)\nu^m \tag{76}$$

Table 1
References used for the experimental data.

#	Reference	Fiber	Matrix
1	[59,73]	Carbon	Epoxy
2	[60]	Glass	Epoxy
3	[60] [a]	Glass	Epoxy
4	[74]	Polyethylene	Epoxy
5	[61]	Carbon	Epoxy
6	[61]	Carbon	Epoxy
7	[61]	Glass	Epoxy
8	[61]	Glass	Epoxy
9	[62] [b]	Glass	Epoxy
10	[63] [c]	Carbon	Epoxy
11	[64]	Carbon	Epoxy
12	[65] [d]	Carbon	Epoxy
13	[66] [d]	Carbon	Epoxy
14	[67]	Glass	Epoxy
15	[68]	Carbon	Epoxy
16	[68]	Carbon	Epoxy
17	[68]	Carbon	Epoxy
18	[68]	Glass	Epoxy
19	[68]	Glass	Epoxy
20	[12]	Carbon	Epoxy
21	[12]	Carbon	Epoxy
22	[12]	Carbon	Epoxy
23	[12]	Glass	Epoxy
24	[69]	Carbon	Epoxy
25	[70] [d]	Carbon	Epoxy

[a] Supplementary data for fiber and matrix are obtained from #7 and #2, respectively.
[b] Fiber properties are from #19.
[c] Supplementary data for fiber is obtained from #22.
[d] Fiber and matrix properties are from #20.

Table 2
Calibrated parameters for the ROMm.

x_1	x_2	x_3
2.0930	−1.4359	0.0059
x_4	x_5	x_6
2.3145	−1.6043	−0.4199
x_7	x_8	x_9
1.7906	−0.9657	0.0065

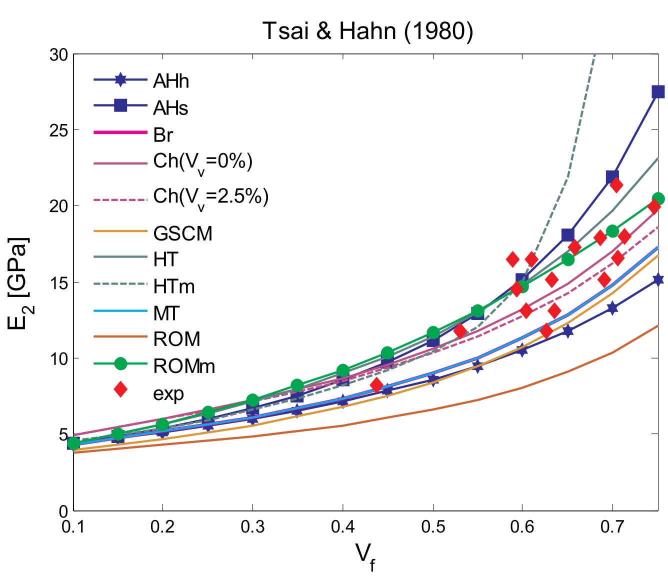

Fig. 2. Example of the most traditional approach in micromechanics to compare models' predictions with experimental data from Ref. [60].

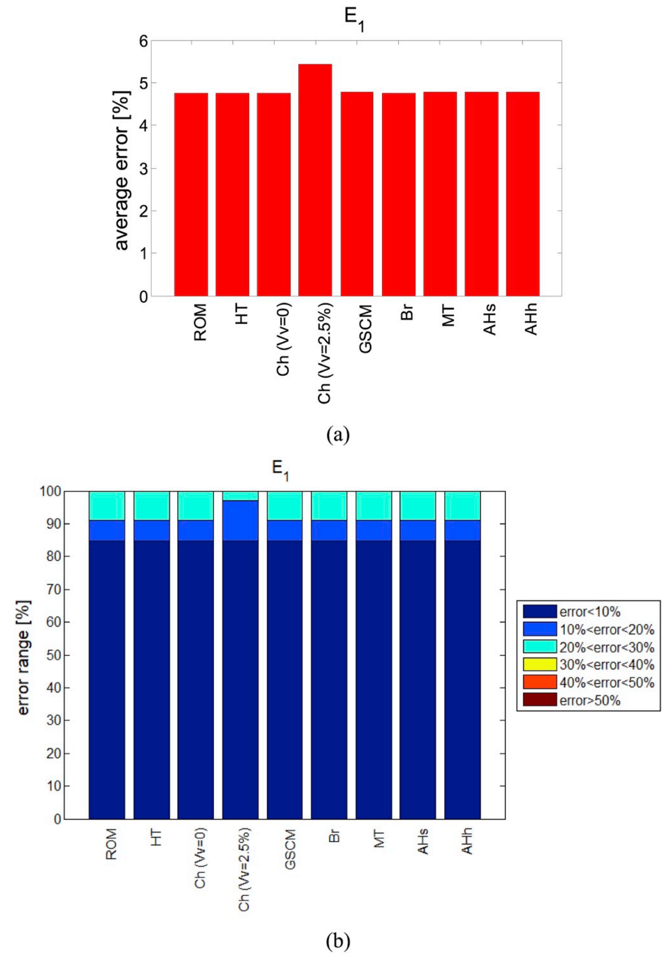

Fig. 3. Results for the longitudinal elastic modulus, E_1: (a) average error; (b) ranges of error.

$$E_2 = \frac{\left[V_f + (1-V_f)a_{11}\right]\left[V_f + (1-V_f)a_{22}\right]}{\left[V_f + (1-V_f)a_{11}\right]\left[\left(\frac{V_f}{E_2^f}\right) + \left(\frac{1-V_f}{E^m}\right)a_{22}\right] + V_f(1-V_f)\left[\left(\frac{\nu_{12}^f}{E_1^f}\right) + \left(\frac{\nu^m}{E^m}\right)\right]a_{12}} \tag{77}$$

$$G_{12} = \frac{V_f + (1-V_f)a_{66}}{\left(V_f/G_{12}^f\right) + \left[(1-V_f)a_{66}/G^m\right]} \tag{78}$$

$$G_{23} = \frac{V_f + (1-V_f)a_{22}}{\left(V_f/G_{23}^f\right) + \left[(1-V_f)a_{22}/G^m\right]} \tag{79}$$

where

$$a_{11} = E^m/E_1^f \tag{80}$$

$$a_{22} = 0.3 + 0.7\left(E^m/E_2^f\right) \tag{81}$$

$$a_{66} = 0.3 + 0.7\left(G^m/G_{12}^f\right) \tag{82}$$

$$a_{12} = \left(\frac{E_1^f \nu^m - E^m \nu_{12}^f}{E_1^f - E^m}\right)(a_{11} - a_{22}) \tag{83}$$

[49] also used the simplified version of the Bridging model. Here, the Bridging model is named as the one represented by Eq.75–83.

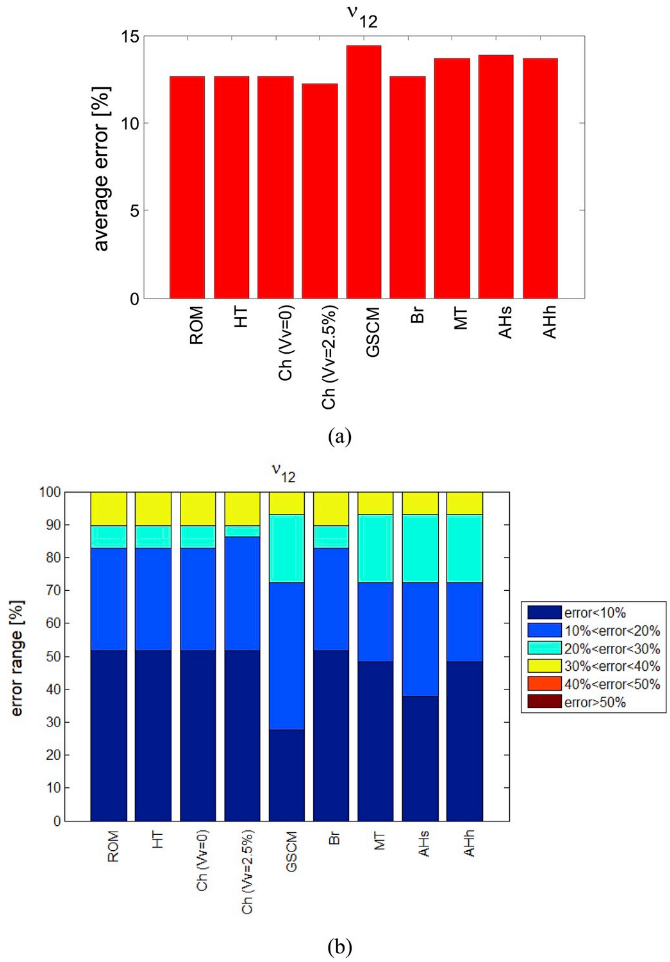

Fig. 4. Results for the in-plane Poisson' ratio, ν_{12}: (a) average error; (b) ranges of error.

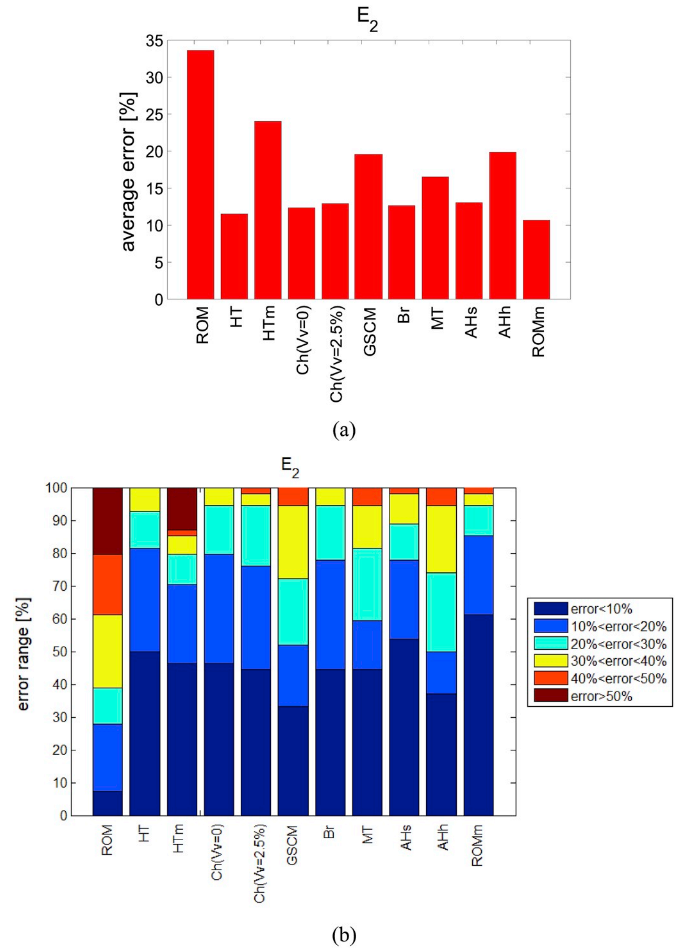

Fig. 5. Results for the transversal elastic modulus, E_2: (a) average error; (b) ranges of error.

3.4. Asymptotic homogenization – square (AHs) and hexagonal (AHh) symmetries

The asymptotic homogenization technique is very popular in composite modeling due to its rigorous mathematical basis [16,17,27]. For the effective elastic properties [16], presented an analytical solution considering square symmetry and isotropic constituents [50]. extended this approach for transversally isotropic fibers using analytical solutions that are not in a closed-form [51]. also considered transversally isotropic fiber but with hexagonal symmetry pattern. A brief introduction about the asymptotic homogenization technique is presented in the sequence based on [16].

The homogenization modeling procedure assumes a two scale approach with macroscopic and microscopic variables, x_i and $y_i = x_i/\varepsilon$, respectively, with $\varepsilon \to 0$. Hence, $\partial/\partial x_i \to [(\partial/\partial x_i) + (1/\varepsilon)(\partial/\partial y_i)]$. The essential assumption is that displacement, strain and stress fields may be defined as an asymptotical series in powers of small parameter ε

$$u_i^{(\varepsilon)} = u_0^{(\varepsilon)}(\mathbf{x}) + \varepsilon u_1^{(\varepsilon)}(\mathbf{x},\mathbf{y}) + \ldots \tag{84}$$

$$e_{ij}^{(\varepsilon)} = e_{ij}^{(0)}(\mathbf{x},\mathbf{y}) + \varepsilon e_{ij}^{(1)}(\mathbf{x},\mathbf{y}) + \ldots \tag{85}$$

$$\sigma_{ij}^{(\varepsilon)} = \sigma_{ij}^{(0)}(\mathbf{x},\mathbf{y}) + \varepsilon \sigma_{ij}^{(1)}(\mathbf{x},\mathbf{y}) + \ldots \tag{86}$$

Based on that, the following expressions can be written for each power of ε

$$e_{ij}^{(0)}(\mathbf{x},\mathbf{y}) = \frac{1}{2}\left(\frac{\partial u_i^{(0)}}{\partial x_j} + \frac{\partial u_j^{(0)}}{\partial x_i}\right) + \frac{1}{2}\left(\frac{\partial u_i^{(1)}}{\partial y_j} + \frac{\partial u_j^{(1)}}{\partial y_i}\right) \tag{87}$$

$$e_{ij}^{(1)}(\mathbf{x},\mathbf{y}) = \frac{1}{2}\left(\frac{\partial u_i^{(1)}}{\partial x_j} + \frac{\partial u_j^{(1)}}{\partial x_i}\right) + \frac{1}{2}\left(\frac{\partial u_i^{(2)}}{\partial y_j} + \frac{\partial u_j^{(2)}}{\partial y_i}\right) \tag{88}$$

$$\sigma_{ij}^{(0)}(\mathbf{x},\mathbf{y}) = c_{ijkl}(\mathbf{y})\frac{\partial u_k^{(0)}}{\partial x_j} + c_{ijkl}(\mathbf{y})\frac{\partial u_k^{(1)}}{\partial y_j}$$

$$\sigma_{ij}^{(1)}(\mathbf{x},\mathbf{y}) = c_{ijkl}(\mathbf{y})\frac{\partial u_k^{(1)}}{\partial x_j} + c_{ijkl}(\mathbf{y})\frac{\partial u_k^{(2)}}{\partial y_j} \tag{89}$$

Applying on the equilibrium equation, the term of $O(\varepsilon^{-1})$ is

$$\frac{\partial \sigma_{ij}^{(0)}}{\partial y_j} = \frac{\partial c_{ijkl}}{\partial y_j}\frac{\partial u_k^{(0)}}{\partial x_j} + \frac{\partial}{\partial y_j}\left(c_{ijkl}(\mathbf{y})\frac{\partial u_k^{(1)}}{\partial y_j}\right) = 0 \tag{90}$$

since $u_k^{(0)} = u_k^{(0)}(\mathbf{x})$. From this equation, it possible to write that

$$u_i^{(1)}(\mathbf{x},\mathbf{y}) = N_{ikl}(\mathbf{y})\frac{\partial u_k^{(0)}(\mathbf{x})}{\partial x_l} \tag{91}$$

where $N_{ijk}(\mathbf{y})$ is a third order tensor where the components are Y-periodic functions.

Substituting Eq. (91) into Eq. (90) yields the following unit cell problems for determining Y-periodic functions $N_{ikl}(\mathbf{y})$:

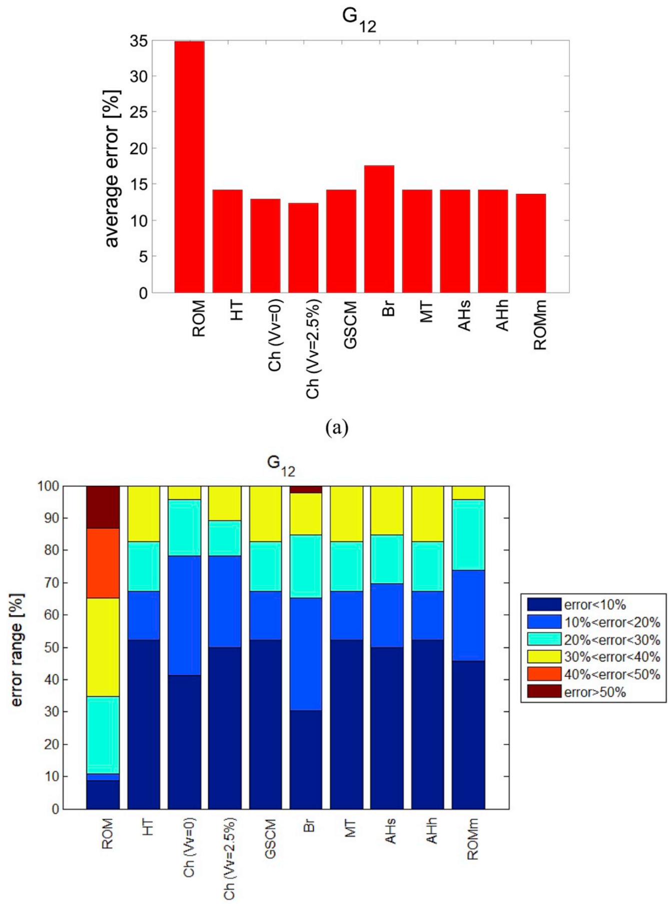

(b)

Fig. 6. Results for the in-plane shear modulus, G_{12}: (a) average error; (b) ranges of error.

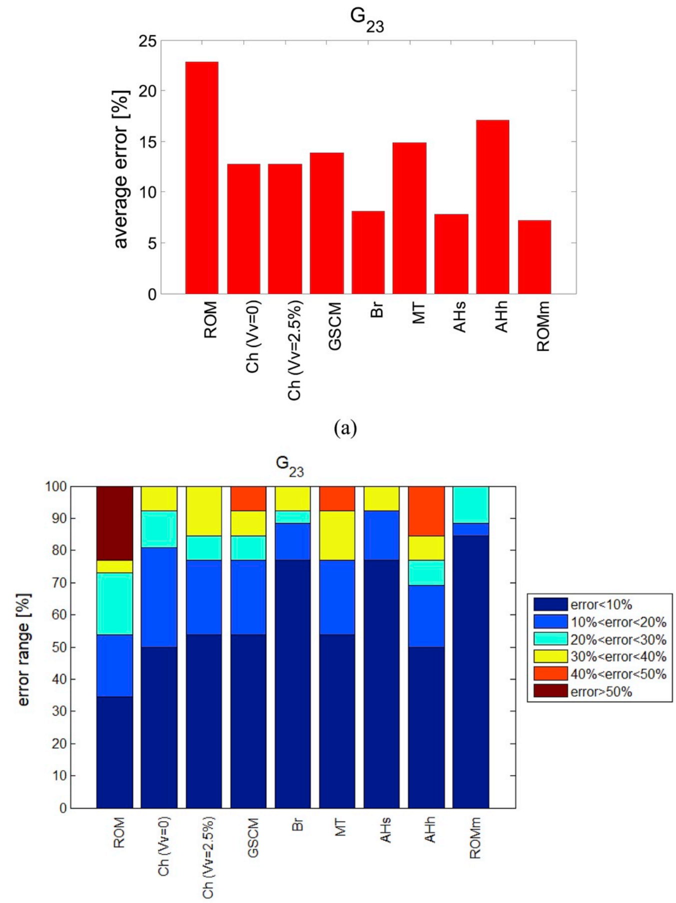

(b)

Fig. 7. Results for the out-of-plane shear modulus, G_{23}: (a) average error; (b) ranges of error.

$$\frac{\partial}{\partial y_j}\left(c_{ijmn}(\mathbf{y})\frac{\partial N_{\mathrm{mkl}}(\mathbf{y})}{\partial y_n}\right) = -\frac{\partial c_{ijkl}}{\partial y_j} \tag{92}$$

Using the terms of $O(\varepsilon^0)$ and integrating over the unit cell domain, the effective elastic tensor is defined by

$$\tilde{c}_{ijkl} = \frac{1}{|Y|}\int\left[c_{ijkl}(\mathbf{y}) + c_{ijmn}(\mathbf{y})\frac{\partial N_{mkl}(\mathbf{y})}{\partial y_n}\right]d\mathbf{y} \tag{93}$$

By analyzing Eq. (92), it is evident that the problem is to obtain $N_{mkl}(\mathbf{y})$. These functions are obtained solving six independent problems: two anti-plane strain problems, for the cases of shear with the longitudinal direction and one of the transversal ones; and four plane strain problems, for the other cases.

According to Ref. [52]; the infinite series may be properly truncated on the second term with sufficient accuracy and just one set of equations is required for both symmetries, square and hexagonal; what define the symmetry adopted is the parameter a. The following equations are used to compute the elastic properties for the asymptotic homogenization model

$$k = k_f V_f + k_m(1 - V_f) - \frac{V_f(k_m - k_f)^2 K}{m_1} \tag{94}$$

$$l = l_f V_f + l_m(1 - V_f) - \frac{V_f(k_m - k_f)(l_m - l_f)K}{m_1} \tag{95}$$

$$n = n_f V_f + n_m(1 - V_f) - \frac{V_f(l_m - l_f)^2 K}{m_1} \tag{96}$$

$$p = p_m - 2V_f p_m P \tag{97}$$

$$m = m_m - V_f(m_m - m_f)M \tag{98}$$

$$m' = m_m - V_f(m_m - m_f)M' \tag{99}$$

where

$$K = C\left\{V_m + \frac{(2a-1)(1+\kappa_m)CR^{4a}(S_{2a})^2}{B^{-1} + R^{4a-2}\left[AB^{-1}r + g + (2a-1)DR^2(S_{2a})^2\right]}\right\} \tag{100}$$

$$P = \frac{\chi_p}{\left[1 + V_f\chi_p - (2a-1)\chi_p{}^2R^{4a}(S_{2a})^2\right]} \tag{101}$$

$$M = \frac{1+\kappa_m}{\left[1 + \kappa_m(m_f/m_m)\right](1 + R^2H^- - I)} \tag{102}$$

$$M' = \frac{1+\kappa_m}{\left[1 + \kappa_m(m_f/m_m)\right](1 + R^2H^+ - I')} \tag{103}$$

$$\kappa_{f,m} = 1 + 2(m_{f,m}/k_{f,m}) \tag{104}$$

$$\chi_p = \frac{p_m - p_f}{p_m + p_f} \tag{105}$$

$$H^+ = Ar_1 + B\kappa_m\frac{\pi}{\sin(\pi/a)} + (3-a)B\left[\left(\frac{5S_4}{\pi}\right) + g_1\right] \tag{106}$$

$$H^- = Ar_1 + B\kappa_m \frac{\pi}{\sin(\pi/a)} - (3-a)B\left[\left(\frac{5S_4}{\pi}\right) + g_1\right] \tag{107}$$

$$I = \begin{cases} \dfrac{R^{12}(Ar_2 - Bg_2)(Ar_3 - Bg_3)}{1 + R^{10}(Ar_4 - Bg_4)} & if \quad a = 2 \\ \dfrac{3R^8B^2\left(15R^2S_6 - 4T_5\right)^2}{1 + 100R^{12}A(S_6)^2} & if \quad a = 3 \end{cases} \tag{108}$$

$$I' = \frac{R^{12}(Ar_2 + Bg_2)(Ar_3 + Bg_3)}{1 + R^{10}(Ar_4 + Bg_4)} \tag{109}$$

$$r = \beta_{4a-1}^{2a-1}\beta_{4a-1}^{2a+1}R^{4a+2}(S_{4a})^2 \tag{110}$$

$$r_1 = (2a-1)(S_{2a})^2R^{4a-2} \tag{111}$$

$$r_2 = \beta_3^3\beta_7^5R^6S_4S_8 \tag{112}$$

$$r_3 = \beta_3^1\beta_7^3R^6S_4S_8 \tag{113}$$

$$r_4 = \beta_7^3\beta_7^5R^6(S_8)^2 \tag{114}$$

$$g = -(2a-1)\left(R^2\beta_{4a}^{2a}S_{4a} - \beta_{4a-2}^{2a-1}T_{4a-1}\right) \tag{115}$$

$$g_1 = -6S_4R^2 \tag{116}$$

$$g_2 = -R^2\beta_8^2S_8 + \beta_6^5T_7 \tag{117}$$

$$g_3 = -5R^2\beta_8^6S_8 + 5\beta_6^5T_7 \tag{118}$$

$$g_4 = -5R^2\beta_{12}^6S_{12} + 5\beta_{10}^5T_{11} \tag{119}$$

$$A = \frac{\left[\kappa_m\left(m_f/m_m\right) - \kappa_f\right]}{\left[\left(m_f/m_m\right) + \kappa_f\right]}B \tag{120}$$

$$B = \frac{\left[1 - \left(m_f/m_m\right)\right]}{\left[1 + \kappa_m\left(m_f/m_m\right)\right]} \tag{121}$$

$$C = \frac{m_m}{\left[m_m + k_mV_f + k_f\left(1 - V_f\right)\right]} \tag{122}$$

$$D = 2[(k_2/k_1) - 1]C \tag{123}$$

$$\beta_k^l = \frac{k!}{l!(k-l)!} \tag{124}$$

$$S_4 = \begin{cases} 3.1512120 & if \quad a = 2 \\ 0 & if \quad a = 3 \end{cases} \tag{125}$$

$$S_6 = \begin{cases} 0 & if \quad a = 2 \\ 5.8630316 & if \quad a = 3 \end{cases} \tag{126}$$

$$S_8 = \begin{cases} 4.2557731 & if \quad a = 2 \\ 0 & if \quad a = 3 \end{cases} \tag{127}$$

$$S_{12} = \begin{cases} 3.9388490 & if \quad a = 2 \\ 6.00096399 & if \quad a = 3 \end{cases} \tag{128}$$

$$T_5 = \begin{cases} 0 & if \quad a = 2 \\ 5.6568027 & if \quad a = 3 \end{cases} \tag{129}$$

$$T_7 = \begin{cases} 4.5155155 & if \quad a = 2 \\ 0 & if \quad a = 3 \end{cases} \tag{130}$$

$$T_{11} = \begin{cases} 3.8807309 & if \quad a = 2 \\ 6.0301854 & if \quad a = 3 \end{cases} \tag{131}$$

with $a = 2$ for square symmetry and $a = 3$ for hexagonal symmetry.

The non-null components of the elastic tensor are computed by

$$c_{1122} = c_{2211} = c_{1133} = c_{3311} = l \tag{132}$$

$$c_{1111} = n \tag{133}$$

$$c_{2222} = c_{3333} = k + m' \tag{134}$$

$$c_{2233} = c_{3322} = k - m' \tag{135}$$

$$c_{2323} = c_{2332} = c_{3223} = c_{3232} = m \tag{136}$$

$$c_{1212} = c_{1221} = c_{2112} = c_{2121} = c_{1313} = c_{1331} = c_{3113} = c_{3131} = p \tag{137}$$

Some additional examples of application of asymptotic homogenization to obtain effective properties are presented by Refs. [53,54]; where the interphase influence is included, [55]; which studied thermal properties, and [56] that presented a numerical procedure for displacement field computation.

4. Results

This Section applies different micromechanics models to obtain equivalent effective macroscopic properties. The models discussed on the preceding section are employed for this aim. The main objective is to establish a comparison with experimental data. In this regard, it should be pointed out that experimental data of composite materials have high uncertainty values due to irregular fiber arrangement. For instance, the fiber and matrix storage may have significantly influence on the cure process, inducing fiber misalignment, voids, residual stress and shape distortion [57]. An extensive discussion about modeling manufacture process of composite materials, not restrict just for unidirectional laminates, is presented by Ref. [58].

The comparison with experimental data considers the following set of experiments compiled from the literature: 33 data for E_1, 54 data for E_2, 46 data for G_{12}, 26 data for G_{23} and 29 data for ν_{12}. The references for these data are presented in Table 1, as well as the type of fiber and matrix. The calibrated parameters of the novel ROMm are presented in Table 2.

The most traditional form to compare different micromechanical models with experimental data is plot the effective property according to the fiber volume fraction. The experimental results are plotted together with markers. However, this graphic only can be useful for qualitative comparison. Fig. 2 shows a comparison between all the analytical models and a set of experimental data. It is impossible to allege, in a quantitative sense, which model obtain the best prediction. Moreover, if the comparison includes a broad range of fibers and matrices types, many figures are required.

The comparison considers two different approaches for each effective property: the absolute value of the average error, which one is able to present the general estimative; and the ranges of error, that are classified as smaller than 10%, between 10% and 20%, between 20% and 30%, between 30% and 40%, between 40% and 50% and higher than 50%.

Fig. 3 and Fig. 4 present results of E_1 and ν_{12}, respectively. It should be pointed out that for most of the models based on the ROM, they employ the same estimative of the ROM and therefore, they are not presented in the comparison. Two main conclusions may be highlighted:

i) all the models obtained a good approximation for E_1, once the constituents work very similar to elements in parallel for longitudinal loads (at least in elastic regime);
ii) despite all the models also get closer predictions for ν_{12}, the Chamis model obtained a small improvement when the void volume fraction is considered, indicating a possible modeling improvement;
iii) an experimental measurement of ν_{12} has many dificults, for instance due to material inomogeneity, and the data are very scattered;
iv) since all the models' prediction are acurate for E_1 and none of the presented a significant improvement for ν_{12}, the most recomendable estimation for these properties are those presented in Eq.(1) and (2) by the ROM due to its simplicity.

For the other properties the conclusions are discussed individually because the ROMm is also included and a more significant disagreement between models' prediction is realized. For the transversal elastic modulus, E_2, results are presented in Fig. 5. The following points are highlighted:

i) for E_2 the ROMm obtained the best prediction in both methodology with the average error equal to 10.6% and 61.1% of the estimations with error smaller than 10% compared with the experimental data;
ii) the modification of the HT model, HTm, do not present an improvement on the original model capability;
iii) the AHs obtained closer predictions of the experimental data than AHh, indicating that the methodology proposed by Ref. [8]; where an initially square array is modified according to the degree of nonuniformity, may be very relevant for numerical simulation;
iv) once the fiber distribution is highly influenced by manufacture process, uncertainty quantification related to the degree of nonuniformity of each manufacture process seem to be a promising improvement in relation to the traditional finite element procedures.

For the in-plane shear modulus, G_{12}, results are presented in Fig. 6 and the main conclusions are:

i) for G_{12} all the models have a very close prediction, indicating that the influence of the fiber distribution has not a considerable influence in this property;
ii) it is well know the nonlinear behavior of unidirectional laminae for high in-plane shear stress-strain level [71], becoming a hard task properly measure G_{12} and, consequently, it is expected higher error for this properties;
iii) due to this nonlinearity, the micromecanical elastic modulus discussed in this paper must be considered for lower in-plane shear stress-strain level;
iv) as a consequence of this issue, the models based on the ROM obtained a closer prediction than thoses elasticity-based once the novel ROMm and HT contain calibrated parameters and Ch has a semi-empirical basis proposed also to adjust the estimation according to experimental data.

Finally, for out-of-plane shear modulus, G_{23}, the following conclusions are pointed out:

i) for G_{23} the ROMm obtained the best agreement with experimental data, where the average error is equal to 7.19% and 84.6% of the prediction has a error smaller than 10%;
ii) the Br and AHs also have an excelent estimations for G_{23}, both with average error smaller than 10% and more than 75% of the cases with error smaller than 10%;
iii) smaller amount of experimental data for G_{23} is reported on the literature because the most traditional modeling procedure for laminate plates, the Classical Laminate Theory, assumes plane-stress in each layer [71];
iv) with the advantage of computational tools, through thickness effecst have been regarded and its influence in laminate failure becomes more relevant to modeling delamination and notched plates, for example [72];
v) as the out-of-plane load can be considered as a biaxial tension-compression equivalent load, include the degree of nonuniformity for numerical modeling also is suggested for further studies.

5. Conclusions

An overview of 10 micromechanical models to estimate the effective elastic properties of unidirectional laminae is presented. Four of these models are based on the ROM and five are elasticity based. Also, a new modified ROM model is proposed. It is formulated by a simple set of equations. This modified ROM model provides the effective macromechanical properties that better agree with the experimental data. Results of 10 micromechanical models are compared with 188 experimental data from 25 references. Among the models, the AHs resulted in the best predictions. The novel ROMm model proves to be an interesting approach but it needs to be adjusted for the specific material. The calibrated parameters are just for carbon and glass fibers with epoxy matrix. Comparing ROMm and AHs, the ROMm has the advantage to be a simple set of equations, but it needs an additional adjustment for different materials. On the other hand, AHs has more complex equations but it does not require any calibration. In summary, ROMm gives the best correlation with the experimental data among the ROM-based models, while AHs presents the best predictions among the elasticity-based models.

Acknowledgements

The authors acknowledge the support of the Brazilian Research Agencies CNPq, CAPES and FAPERJ. The Air Force Office of Scientific Research (AFOSR) and the Natural Sciences and Engineering Research Council of Canada (NSERC) are also acknowledged.

References

[1] Andrianov IV, Awrejcewicz J, Danishevs'kyy VV. Asymptotical mechanics of composites - modelling composites without FEM. Springer; 2018.
[2] Wiggers H, Ferro O, Sales RCM, Donadon MV. Comparison between the mechanical properties of carbon/epoxy laminates manufactured by autoclave and pressurized prepreg. Polym Compos 2018;39:S4.
[3] Shah PD, Melo JDD, Cimini Jr CA, Ridha M. Evaluation of notched strength of composite laminates for structural design. J Compos Mater 2010;44:2381–92.
[4] Tsai SW, Melo JDD. An invariant-based theory of composites. Compos Sci Technol 2014;100:237–43.
[5] Lekhnitskii SG. Theory of elasticity of an anisotropic body. Moscow: Mir; 1981.
[6] Wongsto A, Li S. Micromechanical FE analysis of UD fibre-reinforced composites with fibres distributed at random over the transverse cross-section. Composites Part A 2005;36:1246–66.
[7] Selvadurai APS, Nikopour H. Transverse elasticity of a unidirectionally reinforced composite with an irregular fibre arrangement: experiments, theory and computations. Compos Struct 2012;94:1973–81.
[8] Elnekhaily SA, Talreja R. Damage initiation in unidirectional fiber composites with different degrees of nonuniform fiber distribution. Compos Sci Technol 2018;155:22–32.
[9] Alazwari MA, Rao SS. Modeling and analysis of composite laminates in the presence of uncertainties. Composites Part B 2019;161:107–20.
[10] Hinton MJ, Kaddour AS, Soden PD. Failure criteria in fibre reinforced polymer composites: the world-wide failure Exercise. Elsevier; 2004.
[11] Kaddour AS, Hinton MJ. Maturity of 3D failure criteria for fibre reinforced composites: comparison between theories and experiments: Part B of WWFE-II. J Compos Mater 2013;47:925–66.
[12] Kaddour AS, Hinton MJ, Smith PA, Li S. The background to the third world-wide failure exercise. J Compos Mater 2013;47:2417–26.
[13] Soden PD, Kaddour AS, Hinton MJ. Recommendations for designers and researchers resulting from the world-wide failure exercise. Compos Sci Technol 2004;64:589–604.

[14] Younes R, Hallal A, Fardoun F, Chehade FH. "Comparative review study on elastic properties modeling for unidirectional composite materials", composites and their properties, vol. 17. Capítulo; 2012 [IntechOpen].
[15] Christensen RM. Two theoretical elasticity micromechanics models. J Elast 1998; 50:15–25.
[16] Kalamkarov AL. Composite and reinforced elements of construction. Chichester, N.-Y: Wiley; 1992.
[17] Kalamkarov AL. "Asymptotic homogenization method and micromechanical models for composite materials and thin-walled composite structures", mathematical methods and models in composites. London, UK: Imperial College Press; 2014. p. 1–60.
[18] Buryachenko VA. Micromechanics of heterogeneous materials. New York: Springer; 2007.
[19] Christensen RM. A critical evaluation for a class of micromechanics models. J. Mech. Ph.w. Solids 1990;38:379–404.
[20] Willis JR. The overall elastic response of composite materials. J Appl Mech 1983; 50:1202–9.
[21] Raju B, Hiremath SR, Mahapatra DR. A review of micromechanics based models for effective elastic properties of reinforced polymer matrix composites. Compos Struct 2018;204:607–19.
[22] Rarani MH, Naeini KBK, Mirkhalaf SM. Micromechanical modeling of the mechanical behavior of unidirectional composites - a comparative study. J Reinf Plast Compos 2018;37(16):1051–71.
[23] Bacarreza O, Wen P, Aliabadi MH. In: Aliabadi MH, editor. "Micromechanical modelling of tectile composite", woven composites. College London: Imperial; 2015. p. 1–74.
[24] Richter T,W, Carvalho NV, Pinho ST. Predicting the non-linear mechanical response of triaxial braided composites. Composites Part A 2018;114:117–35.
[25] Kalamkarov AL. On the determination of effective characteristics of cellular plates and shells of periodic structure. Mech Solids 1987;22(2):175–9.
[26] Kalamkarov AL, Andrianov IV, Danishevs'kyy VV. Asymptotic homogenization of composite materials and structures. Trans. ASME, Applied Mechanics Reviews 2009;62(3). 030802-1 – 030802-20.
[27] Kalamkarov AL, Kolpakov AG. Analysis, design and optimization of composite structures. second ed. Chichester, N.-Y: Wiley; 1997.
[28] Jones RM. Mechanics of composite materials. 2 ed. Taylor & Francis; 1999.
[29] Hull D, Clyne TW. An introduction to composites materials. Cambridge University Press; 1996.
[30] Chamis CC. Mechanics of composite materials: past, present, and future. J Compos Technol Res 1989;11:3–14.
[31] Chamis CC, Abdi F, Garg M, Minnetyan L, Baid H, Huang D, Housner J, Talagani F. Micromechanics-based progressive failure analysis prediction for WWFE-III composite coupon test cases. J Compos Mater 2013;47:2695–712.
[32] Mishra A, Naik NK. Inverse micromechanical models for compressive strength of unidirectional composites. J Compos Mater 2009;43:1199–211.
[33] Halpin JC, Tsai SW. Effects of environmental factors on composite materials. AFML-TR; 1969. p. 67–423.
[34] Halpin JC, Kardos JL. The halpin-tsai equations: a review. Polym Eng Sci 1976;16: 344–52.
[35] Giner E, Vercher A, Marco M, Aarango C. Estimation of the reinforcement factor n for calculating the transverse stiffness E2 with the Halpin-Tsai equations using the finite element method. Compos Struct 2015;124:402–8.
[36] Nocedal J, Wright SJ. Numerical optimization. Springer; 1999.
[37] Andrianov IV, Mitushev V. Exact and "exact" formulae in the theory of composites". 2017. arXiv:1708.02137v1 [math-ph].
[38] Christensen RM. Mechanics of composite materials. New York: Dover Publications; 2005.
[39] Zhang D, Waas AM. A micromechanics based multiscale model for nonlinear composites. Acta Mech 2014;225:1391–417.
[40] Sokolnikoff IS. Mathematical theory of elasticity, vol. 2. New York: McGraw-Hill Book Company; 1956.
[41] Benveniste Y. "A new approach to the application of moti-tanaka's theory in composite materials". Mech Mater 1987;6:147–57.
[42] Mori T, Tanaka K. Average stress in matrix and average elastic energy of materials with misfitting inclusions. Acta Metall 1973;21:571–4.
[43] Mura T. Micromechanics of defects in solids. Martinus Nijhoff; 1987.
[44] Pyrz R. Micromechanics of composites. In: Borst R, Sadowski T, editors. Lecture notes on composite materials - current topics and achievements. Springer; 2008.
[45] Abaimov SG, Khudyakova AA, Lomov SV. On the closed form expression of the Mori-Tanaka theory prediction for the engineering constants of a unidirectional fiber-reinforced ply. Compos Struct 2016;142:1–6.
[46] Huang ZM. A unified micromechanical model for the mechanical properties of two constituent composite materials. Part I: elastic behavior. J Thermoplast Compos Mater 2000;13(4):252–71.
[47] Wang YC, Huang ZM. A New Approach to a Bridging Tensor 2015;36(8):1417–31.
[48] Huang ZM, Zhou YX. Strength of fibrous composites. Springer; 2011.
[49] Huang ZM. On micromechanics approach to stiffness and strength of unidirectional composites. J Reinf Plast Compos 2018;0(0):1–30.
[50] Ramos RR, Sabina FJ, Díaz RG, Castillero JB. Closed-form expressions for the effective coefficients of a fiber-reinforced composite with transversely isotropic constituents - I. Elastic and square symmetry. Mech Mater 2001;33:223–35.
[51] Díaz RG, Castillero JB, Ramos RR, Sabina FJ. Closed-form expressions for the effective coefficients of fibre-reinforced composite with transversely isotropic constituents. I: elastic and hexagonal symmetry. J Mech Phys Solids 2001;49: 1445–62.
[52] Castillero JB, Díaz RG, Ramos RR, Sabina FJ, Brenner R. Unified analytical formulae for the effective properties of periodic fibrous composites. Mater Lett 2012;73:68–71.
[53] Andrianov IV, Danishevs'kyy VV, Kalamkarov AL. Micromechanical analysis of fiber-reinforced composites on account of influence of fiber coatings. Composites Part B 2008;39:874–81.
[54] Díaz RG, Ramos RR, Castillero JB. Modeling of three-phase fibrous composite using the asymptotic homogenization method. Mech Adv Mater Struct 2003;10:1–15.
[55] Kalamkarov AL, Andrianov IV, Pacheco PMCL, Savi MA. Asymptotic analysis of fiber-reinforced composites of hexagonal structure. J Multiscale Model (JMM) 2016;7:1650006.
[56] Macedo RQ, Ferreira RTL, Donadon MV, Guedes JM. Elastic properties of unidirectional fiber-reinforced composites using asymptotic homogenization techniques. J Braz Soc Mech Sci Eng 2018;40:255.
[57] Mesogitis TS, Skordos AA, Long AC. Uncertainty in the manufacturing of fibrous thermosetting composites: a review. Composites Part A 2014;57:67–75.
[58] Advani SG, Sozer M. Process modeling in composite manufacturing. second ed. CRC Press; 2010.
[59] Kriz RD, Stinchcomb WW. Elastic moduli of transversely isotropic graphite fibers and their composites. Exp Mech 1979;19:41–9.
[60] Tsai SW, Hahn HT. Introduction to composite materials. Technomic; 1980.
[61] Soden PD, Hinton MJ, Kaddour AS. Lamina properties, lay-up configurations and loading conditions for a range of fibre-reinforced composite laminates. Compos Sci Technol 1998;58:1011–22.
[62] Bledzki AK, Kessler A, Rikard R, Chate A. Determination of elastic constants of glass/epoxy unidirectional laminates by the vibration testing of plates. Compos Sci Technol 1999;59:2015–24.
[63] Yim JH, Gillespie Jr JW. Damping characteristics of 0° and 90° AS4/3501-6 unidirectional laminates including the transverse shear effect. Compos Struct 2000; 50:217–25.
[64] Huang H, Talreja R. Effects of void geometry on elastic properties of unidirectional fiber reinforced composites. Compos Sci Technol 2005;65:1964–81.
[65] Camanho PP, Maimí P, Dávila CG. Prediction of size effects in notched laminates using continuum damage mechanics. Compos Sci Technol 2007;67:2715–27.
[66] Lee J, Soutis C. A study on the compressive strength of thick carbon fibre-epoxy laminates. Compos Sci Technol 2007;67:2015–26.
[67] Benzarti K, Cangemi L, Maso FD. Transverse properties of unidirectional glass/ epoxy composites: influence of fibre surface treatments. Composites Part A 2001; 32(2001):197–206.
[68] Kaddour AS, Hinton MJ. Input data for test cases used in benchmarking triaxial failure theories of composites. J Compos Mater 2012;46:2295–312.
[69] Schaefer JD, Werner BT, Daniel IM. Strain-rate-dependent failure of a toughened matrix composite. Exp Mech 2014;54:1111–20.
[70] Li W, Cai H, Zheng J. Characterization of strength of carbon fiber reinforced polymer composite based on micromechanics. Polym Polym Compos 2014;22:2.
[71] Barbero EJ. Introduction to composite materials design. 3 ed. CRC Press; 2018.
[72] Reddy JN. Mechanics of laminated composite plates and shells: theory and analysis. second ed. CRC Press; 2003.
[73] Huang ZM. Micromechanical prediction of ultimate strength of transversely isotropic fibrous composites. Int. J. Solids and Struct. 2001;38:4147–72.
[74] Wilczyfiski AP, Lewifiski J. Predicting the Properties of Unidirectional Fibrous Composites with Monotropic Reinforcement. Compos. Sci. Technol. 1995;55: 139–43.